ELSEVIER

Polymer 42 (2001) 1837–1848

polymer

www.elsevier.nl/locate/polymer

Synthesis and properties of soluble alternating copoly(amide–imide)s based on 1,2-bis(4-trimellitimidophenoxy)-4-*t*-butylbenzene and various aromatic diamines

Chin-Ping Yang*, Chi-Shu Wei

Department of Chemical Engineering, Tatung University, 40 Chungshan North Road, Section 3, Taipei 104, Taiwan, ROC

Received 27 March 2000; received in revised form 26 June 2000; accepted 17 July 2000

Abstract

A new diimide dicarboxylic acid, 1,2-bis(4-trimellitimidophenoxy)-4-*t*-butylbenzene (**I**), was prepared by the condensation of 1,2-bis(4-aminophenoxy)-4-*t*-butylbenzene (1,2-BAP-*t*BB) and trimellitic anhydride (TMA) at 1:2 molar ratio. The diamine 1,2-BAP-*t*BB was first synthesized from 4-*t*-butylcatechol and *p*-chloronitrobenzene in the presence of potassium carbonate (K_2CO_3) and then reduced by H_2NNH_2 and Pd/C. A series of novel poly(amide–imide)s (PAIs) III_a–III_k with inherent viscosities of 0.83–1.73 dl/g was prepared from the diimide–diacid **I** with various aromatic diamines (II_a–II_k) by direct polycondensation in a medium consisting of *N*-methyl-2-pyrrolidone (NMP) (as a solvent), triphenyl phosphite/pyridine (as condensing agents), and calcium chloride. Most of the polymers show excellent solubility in amide-type solvents such as NMP and *N,N*-dimethylacetamide (DMAc) and formed a tough, transparent, and flexible film by casting from DMAc solution. The films have tensile strengths of 87–108 MPa, elongations at break of 8–17%, and initial moduli of 2.1–2.6 GPa. The glass transition temperature of these polymers is in the range of 234–276°C and the 10% weight loss temperature is above 475°C in air or in nitrogen.

Keywords: 1,2-bis(4-trimellitimidophenoxy)-4-*t*-butylbenzene; Alternating copoly(amide-imide)s; Solubility

1. Introduction

Aromatic polyimides (PIs) have earned a reputation as high-performance materials as a result of their excellent thermal stability, chemical resistance, and outstanding mechanical properties [1–4]. However, poor handling and intractable characteristics have been major problems due to their high melting point and insolubility. To overcome this drawback, several copolymers have been developed, among them being poly(amide–imide)s (PAIs), whose amide groups can improve the solubility. Therefore, the synthesis of PAIs can offer a compromise between excellent thermal stability and processability.

In our previous studies [5–12], we have successfully applied the phosphorylation polycondensation technique [13–15] to prepare PAIs from imide-containing dicarboxylic acids and aromatic diamines. Compared with the conventional method, this approach provides a significant advantage when smaller quantities are manufactured. Thus, many new series of PAIs could be readily developed by this convenient technique in our laboratory. According to our previous studies [16], the PAIs prepared from the diimide–diacid derived from 1,4-bis(aminophenoxy)-2-*t*-butylbenzene (1,2-BAP-*t*BB) and trimellitic anhydride (TMA) could improve the solubility effectively. Continuing our previous study, the present work tried to synthesize and characterize a series of novel aromatic PAIs using the diimide–diacid derived from non-*para*-linked 1,2-BAP-*t*BB and TMA. It also investigated the effect the *t*-butyl group and *ortho*-oriented phenylene ring with bisether linkages exerted on the solubility, mechanical properties, and thermal properties of these PAIs.

2. Experimental section

2.1. Materials

Trimellitic anhydride (TMA) (Wako) was used as received. The diamine 1,2-bis(4-aminophenoxy)-4-*t*-butylbenzene (1,2-BAP-*t*BB; II_k) was synthesized from 4-*t*-butylcatechol (Acros, 99%) and *p*-chloronitrobenzene (Wako). 1,2-Bis(4-aminophenoxy)benzene (II_h) was synthesized as

* Corresponding author. Tel.: +886-2-2592-5252; fax: +886-2-2586-1939.

E-mail address: cpyang@ttu.edu.tw (C.-P. Yang).

0032-3861/01/$ - see front matter
PII: S0032-3861(00)00589-9

reported [17]. *p*-Phenylenediamine (II_a) (Wako) and *m*-phenylenediamine (II_b) (TCI) were vacuum distilled. Other diamines including 4,4′-oxydianiline (II_c), 4,4′-diaminodiphenyl sulfide (II_d), 4,4′-diaminodiphenylmethane (II_e), 1,4-bis(4-aminophenoxy)benzene (II_f), 1,3-bis(4-aminophenoxy)benzene (II_g), 2,2-bis[4-(4-aminophenoxy)phenyl]propane (II_i), and 2,2-bis[4-(4-aminophenoxy)phenyl]hexafluoropropane (II_j) were all from TCI and used as received.

N,*N*-dimethylacetamide (DMAc; Fluka), *N*,*N*-dimethylformamide (DMF; Fluka), *N*-methyl-2-pyrrolidone (NMP; Fluka) and pyridine (Py; Wako) were purified by distillation under reduced pressure over calcium hydride and stored over 4 Å molecular sieves. Commercially obtained calcium chloride ($CaCl_2$; Wako) was dried under vacuum at 180°C for 6 h. Triphenyl phosphite (TPP; TCI) was used as received.

2.2. Monomer synthesis

2.2.1. 1,2-Bis(4-aminophenoxy)-4-t-butylbenzene (1,2-BAP-tBB)

4-*t*-Butylcatechol (16.6 g; 0.1 mol) was dissolved in 100 ml of DMF before K_2CO_3 (21 g; 0.15 mol) and *p*-chloronitrobenzene (32.3 g; 0.2 mol) were added. The suspension mixture, refluxed at 150–160°C for 8 h with stirring, then allowed to cool and the poured into 120 ml of methanol. The precipitate was isolated by filtration and washed thoroughly with methanol and water. After drying, the crude product was recrystallized with acetic acid to give pure 1,2-bis(4-nitrophenoxy)-4-*t*-butylbenzene (1,2-BNP-*t*BB) in 94% yield; m.p. 148–149°C. A mixture of the obtained dinitro compound made up of 1,2-BNP-*t*BB 37 g, 10% Pd/C (0.12 g), and ethanol (200 ml) was heated to reflux. Then 16 ml of hydrazine hydrate was added dropwise to the suspension solution over a period of 1 h. After complete addition, the mixture was heated at reflux temperature for another 6 h. The reaction solution was then filtered to remove Pd/C. The crude product was recrystallized with ethanol to give colorless needles of 1,2-BAP-*t*BB in 94% yield; m.p. 132–133°C.

IR (KBr): 3422, 3322, 3216 cm^{-1} (N–H str.), 2966 cm^{-1} (aliphatic C–H str.), 1193 cm^{-1} (C–O–C str.). Analysis (wt%): calculated for $C_{22}H_{24}N_2O_2$ (348.44): C, 75.83; H, 6.94; N, 8.04. Found: C, 75.81; H, 6.97; N, 7.84.

^{1}H NMR (400 MHz, $CDCl_3$): δ (ppm) = 6.99 (s, H_a, 1H), 6.97 (d, H_b, 1H), 6.82 (d, H_c, 1H), 6.78 (two overlapped AB doublets, $H_d + H_{d'}$, 4H), 6.58 (two overlapped AB doublets, $H_e + H_{e'}$, 4H), 3.41 (s, $-NH_2$, 4H), 1.23 (s, H_i, 9H). ^{13}C NMR (100 MHz, $CDCl_3$): δ (ppm) = 149.50 (C^6), 149.08 (C^4), 146.90 (C^3), 146.36, 146.06 (C^9, $C^{9'}$), 149.68, 141.36 (C^{12}, $C^{12'}$), 119.96 (C^8), 119.38, 118.68 (C^{10}, $C^{10'}$), 118.43 (C^5), 117.18 (C^7), 115.80, 115.74 (C^{11}, $C^{11'}$), 34.26 (C^2), 31.26 (C^1).

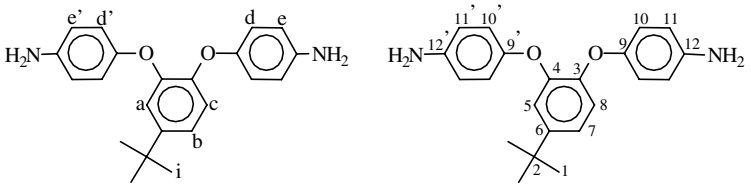

2.2.2. 1,2-Bis(4-trimellitimidophenoxy)-4-t-butylbenzene (I)

A mixture of 6.96 g (20 mmol) of diamine 1,2-BAP-*t*BB and 7.69 g (40 mmol) of TMA was heated to dissolve in dry DMF. Stirring and heating at 40°C were continued for 1 h. Then about 20 ml of toluene was added, and the mixture was heated with reflux for about 6 h until about 1.1 ml of water was distilled off azeotropically. After complete removal of water, the residual toluene was distilled. After cooling, the precipitated yellowish solid was isolated by filtration, washed several times with hot water, and dried in vacuum to yield 13.6 g (98%) of pure diimide–diacid **I**; m.p. 302–304°C.

IR (KBr): 3500–2500 cm^{-1} (carboxyl –OH), 1783, 1717 cm^{-1} (imide C=O), 1096, 723 cm^{-1} (imide ring C–N). Analysis (wt%): calculated for $C_{40}H_{28}N_2O_{10}$ (696.67): C, 68.96; H, 4.05; N, 4.02. Found: C, 68.91; H, 4.10; N, 3.98.

^{1}H NMR (400 MHz, DMSO-d_6): δ (ppm) = 8.38 (d, $H_g + H_{g'}$, 2H), 8.24 (s, $H_f + H_{f'}$, 2H), 8.03 (d, $H_h + H_{h'}$, 2H), 7.39 (two overlapped AB doublets, $H_e + H_{e'}$, 4H), 7.34 (s, H_c, 1H), 7.31 (s, H_a, 1H), 7.20 (d, H_b, 1H), 7.02 (two overlapped AB doublets, $H_d + H_{d'}$, 4H), 1.30 (s, H_i, 9H). ^{13}C NMR (100 MHz, DMSO-d_6): δ (ppm) = 168.00 (C^{20}, $C^{20'}$), 167.40 (C^{19}, $C^{19'}$), 158.72, 158.38 (C^9, $C^{9'}$), 150.52 (C^8), 146.93 (C^3), 146.00 (C^4), 137.62 (C^{15}, $C^{15'}$), 136.65, 136.09 (C^{12}, $C^{12'}$), 133.18 (C^{16}, $C^{16'}$), 130.01 (C^{13}, $C^{13'}$, C^{18}, $C^{18'}$), 127.39 (C^{17}, $C^{17'}$), 127.09 (C^{14}, $C^{14'}$), 124.79, 124.37 (C^{10}, $C^{10'}$), 124.20 (C^7), 122.86 (C^6), 121.03 (C^5), 118.06, 117.35 (C^{11}, $C^{11'}$), 34.35 (C^2), 30.98 (C^1).

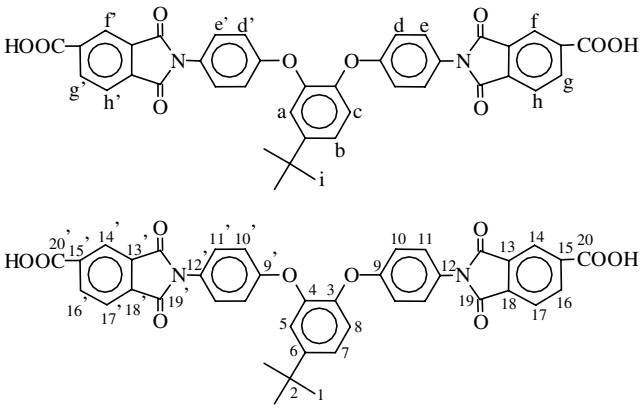

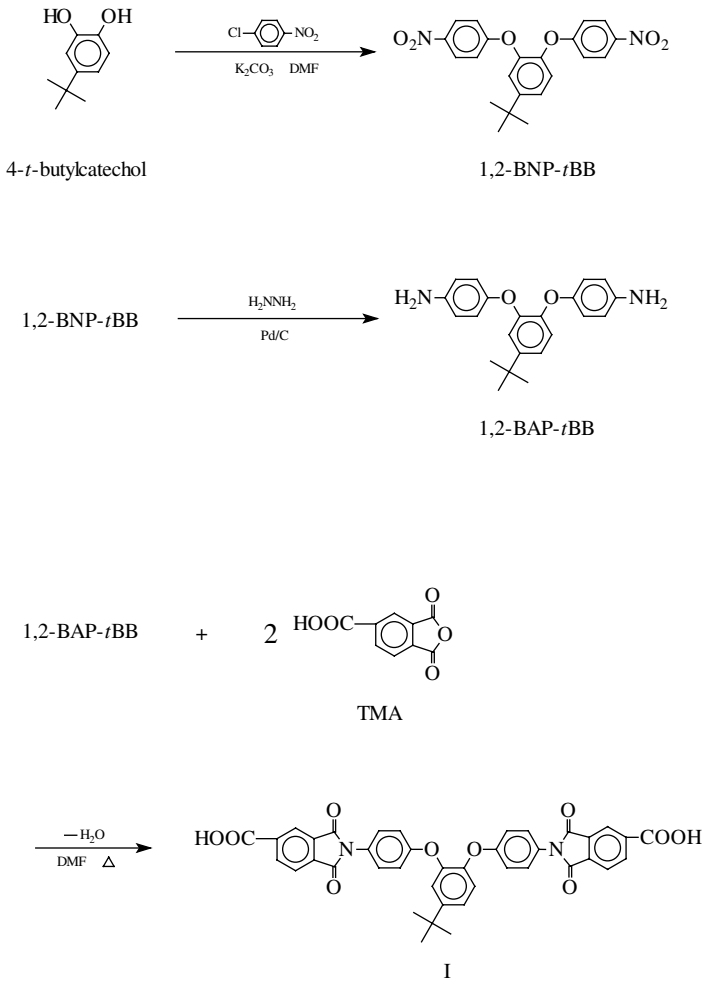

Scheme 1.

2.3. Polymerization

Taking polymer III_i as an example: a mixture of 0.697 g (1.00 mmol) of diimide–diacid (**I**), 0.410 g (1.00 mmol) of diamine II_i, 0.2 g of $CaCl_2$, 0.6 ml of TPP, 1.0 ml of pyridine and 7 ml of NMP were heated with stirring at 100°C for 3 h. The viscous polymer solution obtained was trickled on stirred methanol to give rise to a stringy precipitate which was washed thoroughly with methanol and hot water, collected by filtration, and dried in a vacuum at 100°C. The yield was 1.13 g. The inherent viscosity of the polymer was 1.11 dl/g, as measured on a 0.5 g/dl solution in DMAc at 30°C. The other polymers were prepared following the same procedure.

2.4. Measurements

Elemental analyses were performed on a Perkin–Elmer Model 2400 C, H, N analyzer. ^{1}H and ^{13}C NMR spectra were recorded on a JEOL EX-200 FT-NMR spectrometer. IR spectra were recorded on a JASCO FTIR-7000 Fourier-transform Infrared Spectrometer. The inherent viscosities were measured with a Cannon–Fenske viscometer at 30°C. DSC traces were measured on a SINKU-RIKO DSC-7000 differential scanning calorimeter coupled to a basic component SINKU-RIKO TA-7000 thermal analyzer at the rate of 15°C/min in flowing nitrogen (40 cm^3/min). Thermogravimetry (TG) was conducted with TA Instruments TGA 2050. Experiments were carried out on 10 ± 2 mg samples heated in flowing nitrogen or air (100 cm^3/min) at heating rates of 10 and 20°C/min. An Instron Universal Tester Model 1130 with a load cell of 5 kg was used to study the stress–strain behavior of the polymer film. A gauge of 2 cm and a strain rate of both 5 and 0.5 cm/min were used for this study. Measurements were performed at room temperature with film specimens (0.5 cm wide, 6 cm long, and about 0.5 mm thick) and an average of at least five individual determinations was adopted.

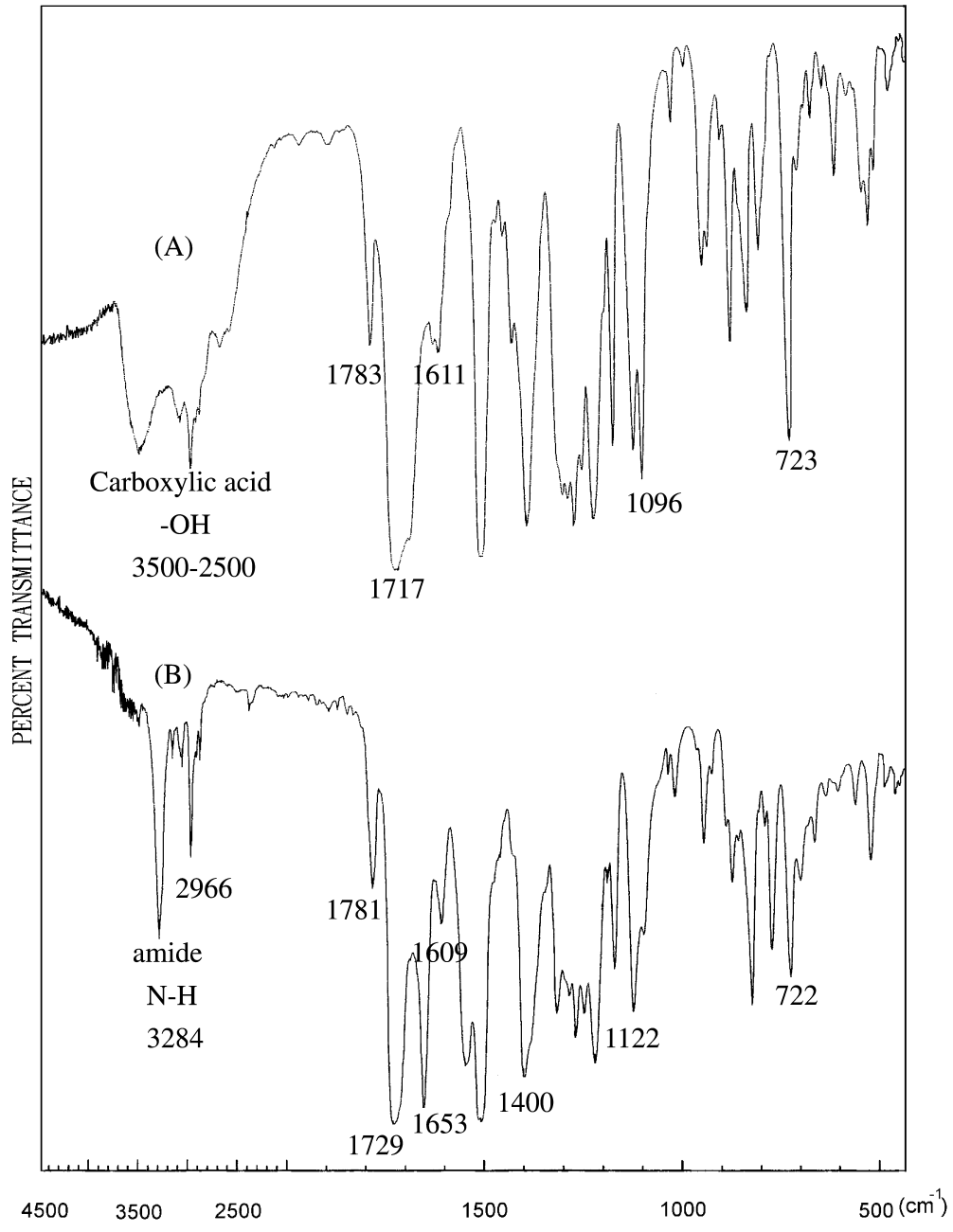

Fig. 1. FT-IR spectra of (A) diimide–diacid **I** and (B) poly(amide–imide) III_a.

3. Results and discussion

3.1. Synthesis

1,2-Bis(4-trimellitimidophenoxy)-4-*t*-butylbenzene (**I**), the diimide–diacid monomer, was prepared via the synthesis of novel bis(ether amine) (1,2-BAP-*t*BB) from 4-*t*-butylcatechol and *p*-chloronitrobenzene in the presence of potassium carbonate (K_2CO_3) to the dinitro compound 1,2-BNP-*t*BB and subsequent reduction; then the produce was via a two-stage procedure that included ring-opening addition of 1,2-BAP-*t*BB with two equivalent amounts of trimellitic anhydride in an amide-type polar solvent to form diamide–tetra-acid, followed by cyclodehydration to the diimide–diacid monomer by means of toluene–water azeotropic distillation (Scheme 1). The chemical structures of 1,2-BAP-*t*BB and diimide–diacid (**I**) were confirmed by elemental analysis and IR, ^1H and ^{13}C NMR spectroscopy, with the results in good agreement with the designed compounds.

The FT-IR characteristic absorptions of 1,2-BAP-*t*BB and diimide–diacid (**I**) are reproduced in Section 2 and Fig. 1A. In the FT-IR spectra, both the characteristic amine absorptions at 3216–3422 cm^{-1} (N–H str.) and the

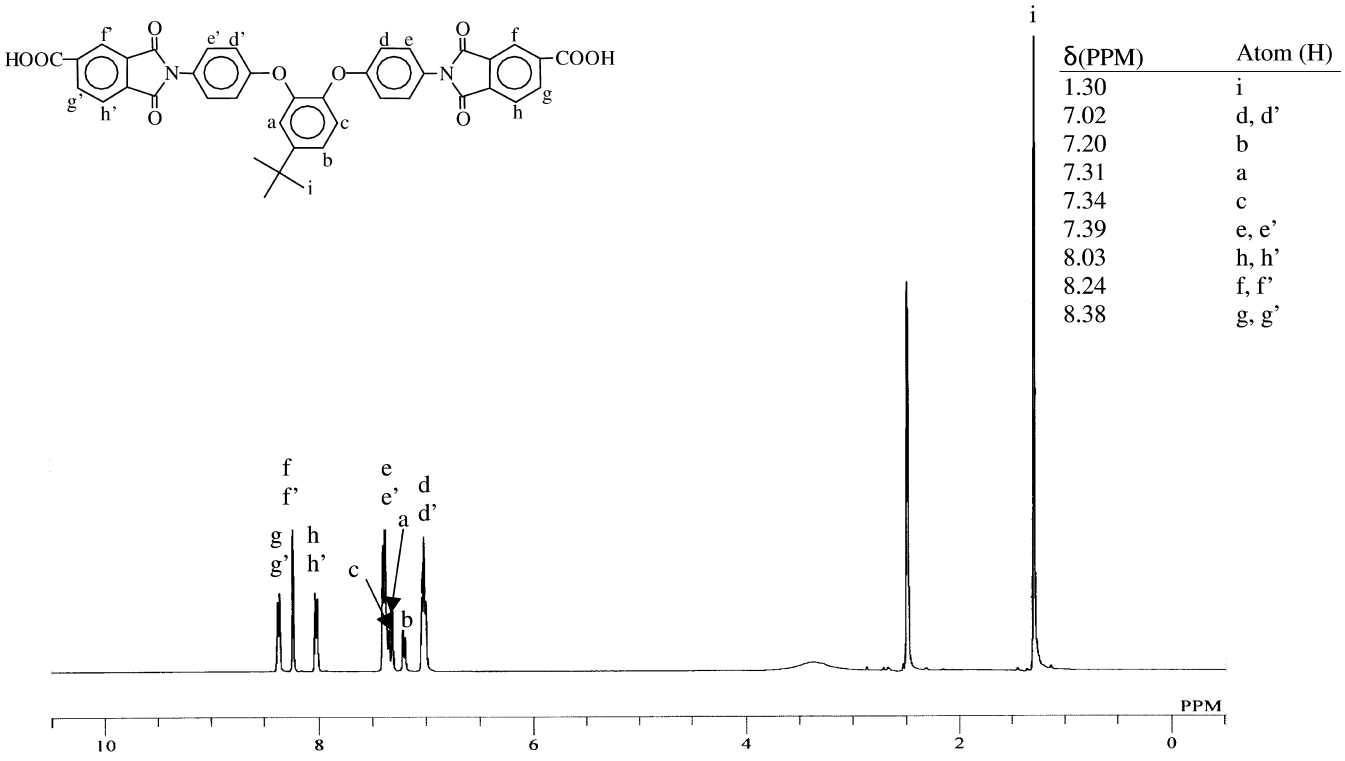

Fig. 2. ^{1}H NMR spectrum of diimide–diacid **I** in DMSO-d_6.

characteristic anhydride absorptions of TMA at 1850 cm^{-1} (asym. C=O), 1776 cm^{-1} (sym C=O), and 1276 cm^{-1} (C–O–C) have disappeared in the IR spectrum of **I** (Fig. 1A). The appearance of the characteristic imide absorptions (1783 and 1717 cm^{-1} (imide C=O), 1096 and 723 cm^{-1} (imide ring C–N)) evidences that the designed diimide–diacid has been synthesized from 1,2-BAP-*t*BB and TMA. The diimide–diacid is confirmed by NMR

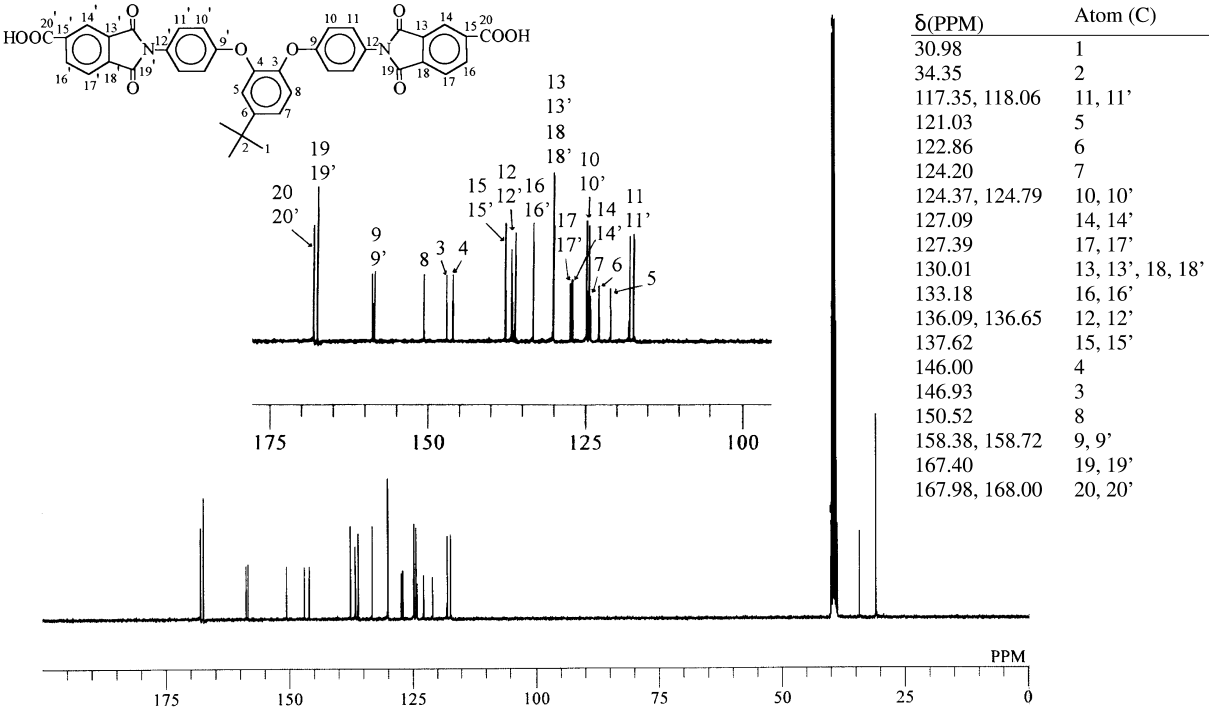

Fig. 3. ^{13}C NMR spectrum of diimide–diacid **I** in DMSO-d_6.

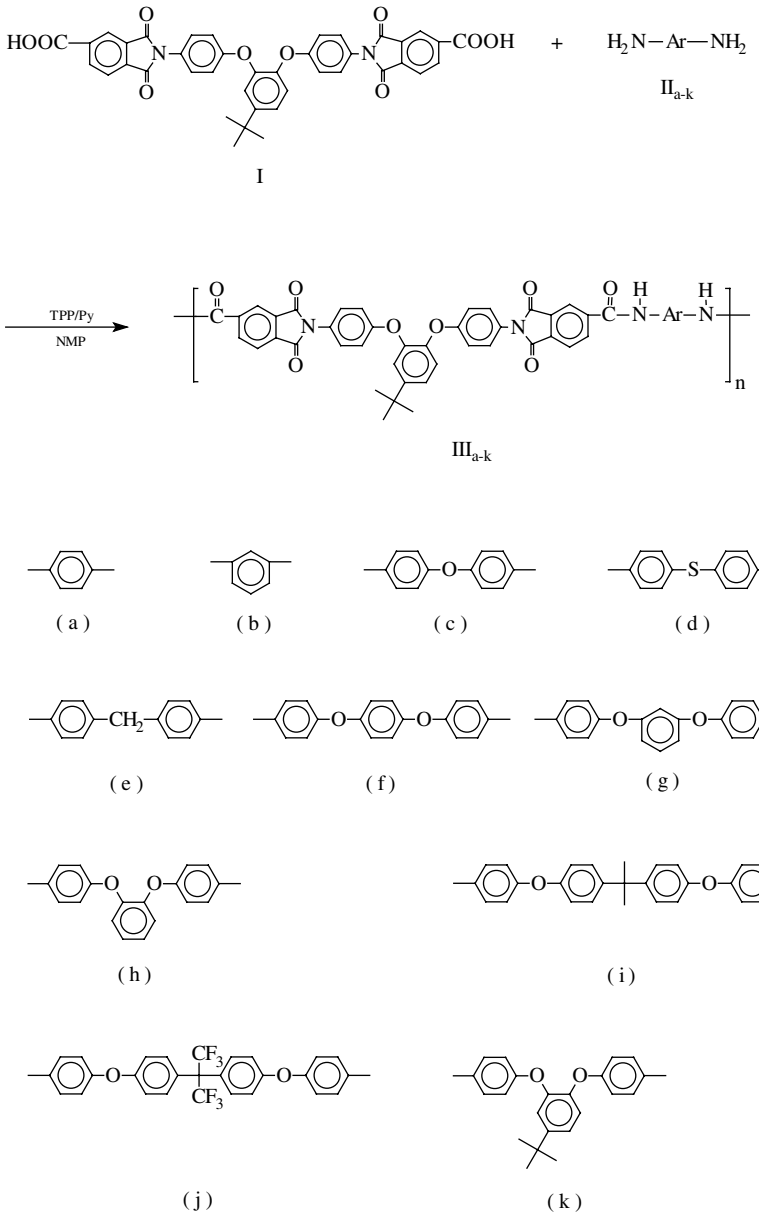

Scheme 2.

spectra again. In the ^{1}H NMR spectrum, all protons of diamine move downfield while 1,2-BAP-*t*BB is transferred to diimide–diacid (**I**) and the aromatic protons (H_e, $H_{e'}$; Fig. 2) at the *ortho* positions of benzene close to the imide group are moved to the farthest downfield especially (from 6.58 ppm of diamine to 7.39 ppm). This phenomenon is due to the inductive effect and the magnetic anisotropy caused by transferring the electron-donating amino groups to the electron-withdrawing imide groups, and the protons of the two oxyphenylene of **I** appear in different shift positions because of the asymmetric structure due to the presence of the *t*-butyl group in the central benzene ring (d and d′, e and e′) and give, like **I**'s precursor diamine monomer, rise to two overlapped AB doublets. Comparing the ^{13}C NMR spectrum of **I** (as shown in Fig. 3) with the spectrum of its precursor 1,2-BAP-**t**BB (Section 2), the ^{13}C absorptions of the central three benzene rings move downfield as a result of the transfer of the electron-donating amino groups to the electron-withdrawing imide groups. From the peaks of the chemical shift in the ^{13}C NMR spectrum, we can clearly observe that the carbons C^{9-12} and $C^{9'-12'}$, the ^{13}C absorptions of two oxyphenylenes which are close to 4-*t*-butylcatechol, are different. However, the C (C^{13}–C^{20}) of a pair of the trimellitimide group which is farther from the center appear almost at the same positions (using 100 MHz NMR), and the 23 peaks of carbons are in agreement with the predictive values.

A series of novel PAIs III_a–III_k was prepared from diimide–diacid **I** and various aromatic diamines II_a–II_k by direct polycondensation using triphenyl phosphite and

Table 1
Synthesis of poly(amide–imide)s

Polymer code	Amounts of reagents used[a]			η_{inh}[b] (dl/g)
	Initial NMP (ml)	$CaCl_2$ (g)	Additional NMP (ml)	
III_a	8.0	0.25	–	0.86
III_b	5.5	0.20	–	0.84
III_c	7.0	0.20	–	1.00
III_d	4.0	0.20	–	0.83
III_e	7.0	0.20	–	0.94
III_f	10.0	0.25	–	1.00
III_g	10.0	0.25	–	0.99
III_h	4.0	0.20	2.0	1.73
III_i	7.0	0.20	–	1.11
III_j	7.0	0.20	–	0.97
III_k	7.0	0.20	–	1.05

[a] Polymerization was carried out with 1 mmol of each monomer, pyridine 1 ml and triphenyl phosphite 0.6 ml at 100°C for 3 h.
[b] Measured at a polymer concentration of 0.5 g/dl in DMAc at 30°C.

pyridine as condensing agents (Scheme 2). Synthesis conditions and inherent viscosities of the PAIs produced are shown in Table 1. Under these conditions the reaction solutions were homogeneously transparent throughout the reaction. The solubility of the polymer and the state of stirring affected the inherent viscosity of the resulting PAI significantly. In general, the molecular weight of the polymer obtained from the phosphorylation reaction is highly dependent on the reactant concentration. According to our earlier reports [5–10], it was repeatedly observed that the higher concentration of the monomer, the higher inherent viscosity provided that no precipitation, or gelation, of the product from the reaction medium took place. It was anticipated that the bulky pendent *t*-butyl group-containing PAIs III_a–III_k with asymmetric main chain structure would have increased solubility in organic solvents and a higher monomer concentration could be tolerated during the polymerization. In some cases, higher molecular weights of the polymers could be obtained by using a higher initial reaction concentration and adding an additional amount of NMP to the highly viscous reaction medium before the formation of swollen gel. The series of PAIs III_a–III_k with inherent viscosities of 0.83–1.73 dl/g was obtained in quantitative yield. All the PAIs could be solution cast into transparent film in DMAc. Except for III_a, III_e, and III_f, all the other PAI films have tough and flexible characteristics, indicating that this series of PAIs have high molecular weights.

The structures of these polymers were confirmed by IR spectroscopy and elemental analysis. A typical IR spectrum for the representative PAI III_a is shown in Fig. 1B. The characteristic absorption bands for the imide ring appear around 1781, 1729 cm^{-1} (imide C=O), 1122, 722 cm^{-1} (imide ring deformation). Absorption bands of the amide groups appear at 3284 and 1653 cm^{-1}. The elemental analysis values of these PAIs are listed in Table 2. In some cases, the values of carbon were found to be lower than the calculated ones for the proposed structures, but the hydrogen values were found to be higher. This may be due to the hygroscopic nature of the amino group. The moisture intake for these PAIs was in the range of 1.40–3.82%. The corrected values were in good agreement with the calculated ones after deducting the amount of moisture intake.

3.2. Properties of polymer

3.2.1. Solubility

The qualitative solubility of the PAIs is shown in Table 3. Most PAIs are soluble in more polar solvents such as NMP, DMAc, DMF and DMSO. This characteristic is due to the fact that both asymmetric *ortho*-oriented phenylene ring and *t*-butyl group contained in the diimide–diacid monomer can overcome the rigid nature of diamine (as III_a), thus forestalling the close packing of polymer chains. Although the PAIs with rigid amide chains, such as III_a, III_c and III_f, are insoluble in less polar solvents like *m*-cresol, pyridine, and tetrahydrofuran (THF), the PAIs with the amide chains (the diamines) which contain diether, asymmetric benzene ring (II_g, II_h, II_k), or soluble groups like isopropylene (II_i, II_j) are readily soluble, even in THF.

3.2.2. Mechanical properties

Transparent films could be cast from the DMAc solutions of all the obtained PAIs. Except for III_a, III_e and III_f, whose films are brittle, the films of all other PAIs have tough and flexible characteristics. Table 4 summarizes the mechanical properties of the PAI films measured at a strain rate of 5 and 0.5 cm/min separately. When the PAI films were measured at the rate of 5 cm/min, five of the films had tensile strengths of 93–103 MPa. All films had strengths-at-break of 87–108 MPa, elongations-at-break of 8–17%, and initial moduli of 2.1–2.6 GPa. For the amide linkage unit (Ar) in polymer backbone, the film is brittle when the structures have either Ar, which has a *para*-oriented phenylene ring like *p*-phenylene (III_a) and biphenylene, or the linkage unit between the multi *para*-oriented phenylene rings is short of

Table 2
Elemental analysis of poly(amide–imide)s

Polymer	Formula (M_w)		Elemental analysis[a] (%)			Moisture intake[b] (%)
			C	H	N	
III_a	$(C_{46}H_{32}O_8N_4)_n$	Calcd	71.87	4.20	7.29	
	$(768.78)_n$	Found	69.46	4.43	7.10	3.35
		Corrected	71.79	4.28	7.34	
III_b	$(C_{46}H_{32}O_8N_4)_n$	Calcd	71.87	4.20	7.29	
	$(768.78)_n$	Found	69.27	4.36	7.19	3.62
		Corrected	71.78	4.20	7.45	
III_c	$(C_{52}H_{36}O_9N_4)$	Calcd	72.22	4.21	6.51	
	(860.88)	Found	71.21	4.44	6.56	1.40
		Corrected	72.21	4.38	6.65	
III_d	$(C_{52}H_{36}O_8N_4S_1)$	Calcd	71.22	4.14	6.39	
	(876.94)	Found	69.90	4.27	6.49	1.85
		Corrected	71.19	4.19	6.61	
III_e	$(C_{53}H_{38}O_8N_4)$	Calcd	74.12	4.46	6.52	
	(858.91)	Found	72.05	4.53	6.48	2.79
		Corrected	74.06	4.40	6.66	
III_f	$(C_{58}H_{40}O_{10}N_4)$	Calcd	73.10	4.23	5.88	
	(952.98)	Found	71.19	4.21	5.84	2.61
		Corrected	73.05	4.10	5.99	
III_g	$(C_{58}H_{40}O_{10}N_4)$	Calcd	73.10	4.23	5.88	2.76
	(952.98)	Found	71.08	4.31	5.99	
		Corrected	73.04	4.19	6.1	
III_h	$(C_{58}H_{40}O_{10}N_4)$	Calcd	73.10	4.23	5.88	
	(952.98)	Found	71.30	4.47	6.00	2.46
		Corrected	73.05	4.36	6.15	
III_i	$(C_{67}H_{50}O_{10}N_4)$	Calcd	75.13	4.70	5.23	
	(1071.15)	Found	73.82	4.74	5.08	1.74
		Corrected	75.10	4.66	5.17	
III_j	$(C_{67}H_{44}O_{10}N_4F_6)$	Calcd	68.25	3.76	4.75	
	$(1179.10)_n$	Found	66.60	3.81	4.90	2.42
		Corrected	68.21	3.72	5.02	
III_k	$(C_{62}H_{48}O_{10}N_4)_n$	Calcd	73.80	4.79	5.55	
	$(1009.\ 08)_n$	Found	70.98	4.68	5.72	3.82
		Corrected	73.69	4.50	5.93	

[a] For C and N: corrected value = found value × (100% + moisture intake%). For H: corrected value = found value × (100% − moisture intake%).
[b] Moisture intake (%)= $(W - W_0) \times 100\%$; W = weight of polymer sample after standing room temperature for three days, and W_0 = weight of the polymer sample after drying in vacuum at 100°C for 10 h.

the flexible property such as III_e and III_f. When the Ar (*p*-phenylene) is substituted with *m*-phenylene, the obtained III_b will have tough characteristic and the maximum strength-at-break will reach up to 108 MPa. For III_c, III_d and III_e contained Ar of two phenylenes, the different characteristics of film arise from the differences in the linkage units though they all have two *para*-oriented phenylenes. The film of III_c with an ether linkage has higher strength but inadequate flexible property and shows unobvious strength-at-yield and less elongation-at-break. However, the film with a sulfur linkage shows obvious strength-at-yield and longer elongation-at-break, indicating that the linkage sulfur is more flexible than oxygen. The film with a methylene linkage between two phenylenes is brittle due to the restricted rotation of its main chain. Furthermore, for the polymers with Ar of triphenylenediether, the *para*-linked III_f is brittle; the *meta*-linked III_g with the central benzene ring shows obvious strength at yield and longer elongation-at-break; the *ortho*-linked III_h and III_k have higher tensile strength and better mechanical properties. III_i and III_j with Ar of four phenylenes containing both the ether linkage and isopropylidene or hexafluoroisopropylidene have not only better solubility but also better flexibility to present strength-at-yield and 15–16% elongation-at-break.

In general, both the lower tensile strength and the longer elongation-at-break can be obtained when a lower strain rate is used. When we operated at a lower strain rate

Table 3
Solubility behavior of poly(amide–imide)s (solubility: measured at a polymer concentration of 0.2 mg/ml in 24 h; +, soluble at room temperature; ±, partially soluble; -S, swelling; −, insoluble

Polymer	Solvent[a]							
	NMP	DMAc	DMF	DMSO	*m*-Cresol	Py	THF	H_2SO_4
III_a	+	+	-S	+	+	+	+	+
III_b	+	+	+	+	+	±	−	+
III_c	+	+	+	+	-S	-S	−	+
III_d	+	+	+	+	+	-S	-S	+
III_e	+	+	+	+	+	-S	−	+
III_f	+	+	-S	+	-S	-S	−	+
III_g	+	+	+	+	+	+	+	+
III_h	+	+	+	+	+	+	+	+
III_i	+	+	+	+	+	+	+	+
III_j	+	+	+	+	+	+	+	+
III_k	+	+	+	+	+	+	+	+

[a] NMP, *N*-methyl-2-pyrrolidone; DMAc, *N*,*N*-dimethylacetamide; DMF, *N*,*N*-dimethylformamide; DMSO, dimethyl sulfoxide; Py, pyridine; THF, tetrahydrofuran.

air and their char yields at 800°C in nitrogen are also tabulated in Table 5. When the PAIs were measured at a heating rate of 20°C/min, their T_{d10}s stayed in the range of 521–538°C in nitrogen and 475–535°C in air.

Sample III_f, for example (as shown in Fig. 4) did not suffer significant weight loss up to about 450°C in nitrogen and in air. The rate of weight loss in N_2 was slower during the early period, whereas it decomposed rapidly at around 550°C. In nitrogen, the rate of weight loss slowed down at about 650°C, and about 50% residual char left at 800°C. One observed unusual phenomenon of oxidative degradation in that the rates of weight loss in air were higher than those in N_2 between 550 and 580°C, but the polymer decomposed rapidly above 600°C and decomposed completely when it was heated to about 730°C. In our previous studies [16], when polymer III_f was compared with isomer IV_f derived from 1,4-bis(aminophenoxy)-2-*t*-butylbenzene, they both showed significant weight loss up to about 450°C in nitrogen or air. Their rates of weight loss in nitrogen were identical

Table 4
Tensile properties of poly(amide–imide) films (films were cast by slow evaporation of polymer solutions in DMAc. The data were measured at strain rates of 5 and 0.5 cm/min (shown in brackets)

Polymer	Strength at yield (MPa)	Strength at break (MPa)	Elongation at break (%)	Initial modulus (GPa)
III_b	– (–)	108 (87)	8 (8)	2.4 (2.4)
III_c	– (–)	105 (101)	8 (9)	2.6 (2.4)
III_d	98 (93)	97 (89)	10 (14)	2.3 (2.1)
III_g	93 (87)	87 (83)	17 (25)	2.1 (2.0)
III_h	– (97)	101 (94)	9 (10)	2.3 (2.1)
III_i	96 (85)	91 (80)	15 (23)	2.3 (2.0)
III_j	101 (94)	90 (87)	16 (25)	2.3 (2.1)
III_k	103 (96)	99 (90)	13 (14)	2.1 (2.0)

(0.5 cm/min) in this study, the result measured is the same as the theoretical one (as shown in Table 4).

3.2.3. Thermal properties

The thermal properties of all the PAIs were evaluated with TGA and DSC, and the results are summarized in Table 5. DSC measurements were conducted at a heating rate of 15°C/min in nitrogen. Quenching from an elevated temperature (about 400°C) to room temperature in air gave predominantly amorphous samples, thus making the glass transition temperatures (T_g) of almost all the PAIs easily observed in the second heating traces of DSC. The T_g values of these PAIs were recorded in the range 234–276°C. This order is correlative to the decreasing order of the stiffness and polarity of the polymer backbones. For example, the T_g of the *p*-diphenoxybenzene-containing III_f is higher than that of its *m*-isomeric III_g, and the perfluoroisopropylidene-containing III_j reveals a higher T_g than its non-fluorinated counterpart III_i.

The thermal stability of the PAIs was characterized by TG analysis conducted at heating rates of 20 and 10°C/min. The temperatures of 10% weight loss (T_{d10}) in nitrogen and

Table 5
Thermal properties of poly(amide–imide)s

Polymer	T_g[a] (°C)	T_{d10}[b] (°C)		Char yield[c] (wt%)
		In N_2	In air	
III_a	273	536 (527)	535	63 (59)
III_b	276	537 (528)	517	57 (52)
III_c	266	530 (515)	500	52 (45)
III_d	270	521 (513)	520	57 (52)
III_e	270	522 (510)	483	54 (48)
III_f	251	527 (516)	489	48 (43)
III_g	234	534 (523)	515	55 (52)
III_h	242	536 (519)	512	51 (46)
III_i	245	525 (518)	500	51 (46)
III_j	251	538 (529)	510	55 (52)
III_k	245	521 (509)	475	48 (43)

[a] Midpoint of baseline shift in the second heating DSC trace with a heating rate of 15°C/min under a nitrogen atmosphere.

[b] Temperatures at which 10% weight loss was recorded by TG at a heating rate of 20 and 10°C/min (shown in brackets).

[c] Residual wt% at 800°C under a nitrogen atmosphere at a heating rate of 20 and 10°C/min (shown in brackets).

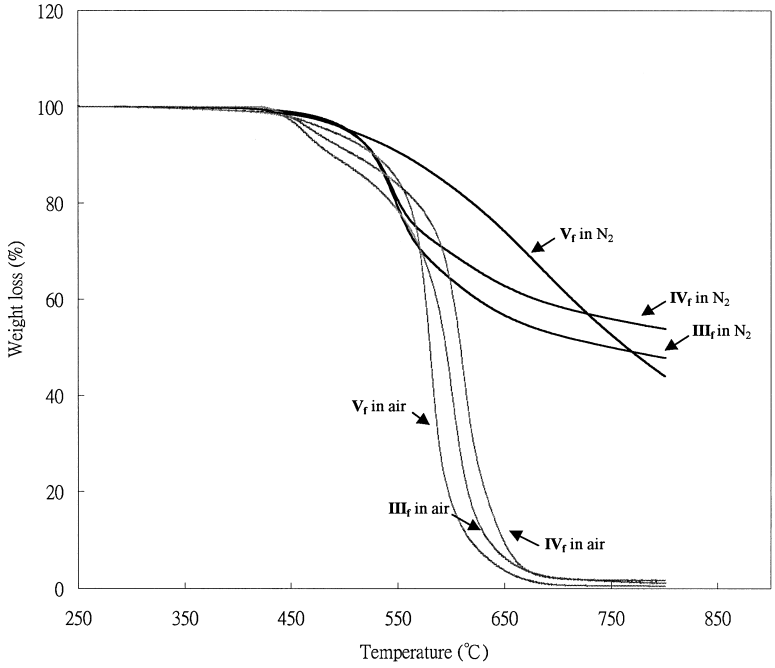

Fig. 4. TG curve for III_f, IV_f and V_f at a heating rate of 20°C/min.

during the early period for the decomposition of the *t*-butyl group. The rate of III_f was higher than that of IV_f when they were heated to about 550°C as a result of the difference in *ortho*- and *para*-oriented phenylene ring. The unusual phenomenon of IV_f was obvious as its rate of decomposition between 550 and 600°C in air was lower than that in nitrogen, and IV_f decomposed rapidly at a temperature slightly higher than III_f did.

Furthermore, we compared III_f with V_f derived from 1,2-bis(4-aminophenoxy)benzene (as shown in Fig. 4). The decomposition rate of V_f, which contains no *t*-butyl group, in air was obviously higher than that in nitrogen. This result did not show any unusual phenomenon; the difference between V_f and the *t*-butyl group-containing PAI (III_f and IV_f) was that V_f decomposed rapidly up to 550°C, although it decomposed slowly during the early period. Therefore, we

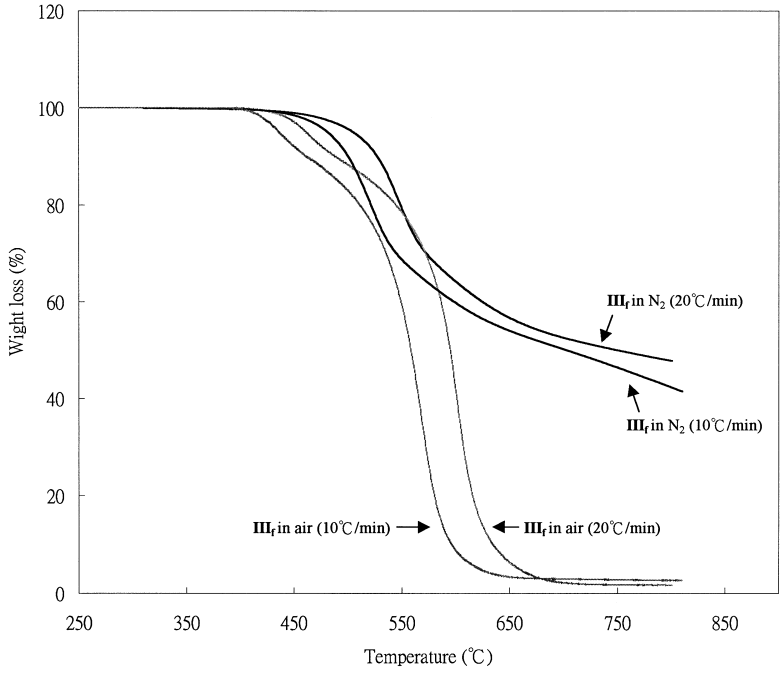

Fig. 5. TG curves for III_f at heating rates of 10 and 20°C/min.

attribute this to the fact that the *t*-butyl group-containing polymers, including III_a–III_k and the series of PAI IV, as reported previously have a slower decomposing rate in air than in nitrogen in high temperature range (between 550 and 600°C) to some possible oxidative interchain crosslinking. The property for heating interchain crosslinking to resist decomposition of the *t*-butyl group-containing PAIs was shown not only in air but also in the char yield at 800°C in nitrogen.

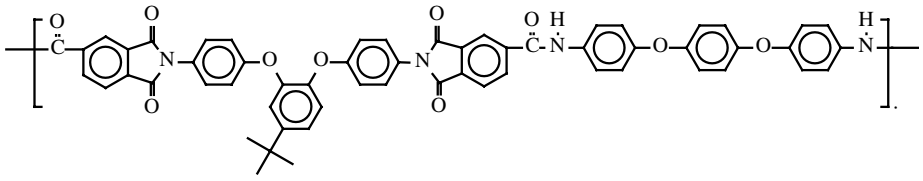

III_f

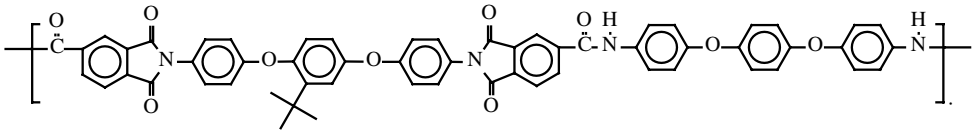

IV_f

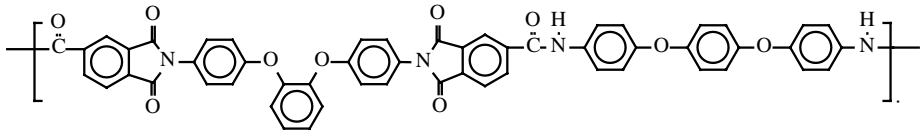

V_f

The temperature of decomposition is affected by the heating rate. When a lower heating rate was used (10°C/min), T_{d10}s measured were lower than the original ones (heating rate of 20°C/min) (as shown in Table 5 and Fig. 5). The phenomenon described above is because the decomposition amount increases with longer time after decomposition; that is, the weight loss of TG analysis is related to both temperature and time.

4. Conclusions

A series of organic solvent-soluble aromatic poly(amide–imide)s with alternating segment, which contains the 1,2-bis(4-phenoxy)-*t*-butylbenzene in main chain, was synthesized by direct polycondensation of 1,2-BAP-*t*BB, TMA with various aromatic diamines using TPP/Py as an activating agent. They had inherent viscosities of 0.83–1.73 dl/g. Most polymers could be cast into transparent and tough (flexible) film, and the cast film exhibited strengths-at-break of 87–108 MPa. The glass transition temperatures of these polymers were in the range 234–276°C. Although their thermal stability was lower than that of either *para*-linked IV series or non-*t*-butyl group-containing V series of PAIs, they still had satisfactory thermal stability when their T_{d10}s were above 475°C in N_2 or in air. The characteristics of the *t*-butyl group, oxidative interchain crosslinking, that the decomposition rate in air while heating was lower in the high temperature range (550–580°C) also showed that the phenomenon was similar to IV series.

Acknowledgements

The authors are grateful to the National Science Council of the Republic of China for support of this work under grant NSC 89-2216-E-036-005.

References

[1] Wilson D, Stenzenberger HD, Hergenrother PM, editors. Polyimides. Glasgow: Blackie and Son, 1990.
[2] Cassidy PE. Thermally stable polymers. New York: Marcel Dekker, 1980.
[3] Feger C, Khojasteh MM, Hroo MS, editors. Advances in polyimide science and technology. Lancaster: Technomic, 1993.
[4] Ghosh KL, Mittal KL, editors. Polyimide, fundamentals and applications. New York: Marcel Dekker, 1996.
[5] Yang CP, Hsiao SH. Makromol Chem 1989;190:2119.
[6] Yang CP, Hsiao SH. J Polym Sci: Polym Chem Ed 1990;28:1149.
[7] Yang CP, Hsiao SH, Chou WL. J Polym Res 1995;2:179.
[8] Yang CP, Lin JH. Polym Int 1995;38:335.
[9] Yang CP, Hsiao SH, Lin JH. J Polym Sci Part A: Polym Chem Ed 1992;30:1865.

[10] Yang CP, Lin JH. Makromol Chem Phys 1995;196:3929.
[11] Yang CP, Hsiao SH, Lin JH. US Patent 5.268.487, 1993.
[12] Yang CP, Hsiao SH, Lin JH. US Patent 5.414.070, 1995.
[13] Yamazaki N, Higashi F. Tetrahedron Lett 1972;28:5074.
[14] Yamazaki N, Higashi F. Tetrahedron 1974;30:1323.
[15] Yamazaki N, Matsumoto M, Higashi F. J Polym Sci: Polym Chem Ed 1975;13:1373.
[16] Yang CP, Hsiao SH, Yang HW. Polym J 1998;30:723.
[17] Yang CP, Cherng JJ. J Polym Sci Part A: Polym Chem Ed 1995;33:2209.